RSC Advances

ROYAL SOCIETY OF CHEMISTRY

www.rsc.org/advances

RSC Advances

ARTICLE

Hydrogel Properties of Electrospun Polyvinylpyrrolidone and Polyvinylpyrrolidone/Poly(acrylic acid) Blend Nanofibers

Daniela Lubasova[a,b], Haitao Niu[b], Xueting Zhao[b], and Tong Lin[b]*

Received 00th January 20xx,
Accepted 00th January 20xx

DOI: 10.1039/x0xx00000x

www.rsc.org/

Hydrogel nanofibers with high water-absorption capacity and excellent biocompatibility offer wide use in biomedical areas. In this study, hydrogel nanofibers from polyvinylpyrrolidone (PVP) and PVP/poly(acrylic acid) (PAA) blend were prepared by electrospinning and by subsequent heat treatment. The effects of post-electrospinning heat treatment and PVP/PAA ratio on hydrogel properties of the nanofibers were examined. Heat treatment at a temperature above 180 °C was found to play a key role in forming insoluble and water-absorbent nanofibers. Both PVP and PVP/PAA nanofibers showed high morphology stability in water and excellent water retention capacity. The swelling ratio of PVP/PAA nanofibers declined with increasing heating temperature and decreasing PVP/PAA unit ratio. In comparison with dense casting films, these nanofiber membranes showed nearly doubled swelling ratio.

Introduction

Hydrogels can absorb significant amount of water and retain their structure integration owing to their hydrophilic three-dimensional polymer network structure. Hydrogels with high water-absorption capacity and good biocompatibility offer wide applications in areas such as wound healing, drug delivery systems, and scaffolds for tissue engineering.[1-4] Nevertheless, most of hydrogels are prepared in the form of dense films or powders. The former is often impermeable to air and liquid, and has lower surface area than porous materials, while the latter is inapplicable to many applications due to the lack of structure integration. Recently, fibrous hydrogels have received considerable attention for their high air/liquid permeability and fast access of water to the internal surface. Hydrogel nanofibers, which are prepared mostly by electrospinning, are of particular interest because of the large surface area and highly porous feature.[5, 6]

Electrospinning is a simple and efficient technique to produce nanofibers.[7, 8] It utilizes a high electrostatic field to generate nanofibers from a fluid. Electrospun nanofibers often show large surface-to-weight (volume) ratio, high porosity, and excellent pore interconnectivity.[9] These unique features allow electrospun nanofibers have extensive applications in diverse areas including filtration, wound healing, cosmetic, energy conversion/storage, and medicine.[10-14]

Hydrogel nanofibers can combine the advantages of both nanofibers and hydrogels. The large surface area of nanofibers enables fast release of antibiotics or growth factors into wound whereas the high porosity of nanofiber mats ensures fast absorption of body fluids and diffusion of waste.[15] Despite the fact that several hydrogel nanofibers, e.g. poly(vinyl alcohol) (PVA),[16] protein,[17] collagen,[18] and poly(N-isopropylacrylamide),[19] have been reported recently, most of the hydrogel nanofibers either are water-soluble due to the lack of sufficient crosslinking[20] or use toxic chemicals as crosslinking agents.[21]

Poly-(N-vinyl-2-pyrrolidone) (PVP) is a water-soluble polymer with excellent biocompatibility. It has high ability to absorb and retain water. Although PVP nanofibers have been reported by a few papers,[22-24] they did not exhibit hydrogel feature due to their high solubility in water. PVP hydrogel membranes have been produced by electrospinning and further crosslinking through UV-C radiation and Fenton reaction.[25] However, fibrous structure was hardly maintained and only a porous membrane was obtained instead after the crosslinking reaction. Moreover, the high energy radiation is often expensive and unavailable readily.

It was reported that PVP and poly(acrylic acid) (PAA) can form strong hydrogen bond interaction.[26] The addition of a small amount of the one mentioned polymer (~10%) to the aqueous solution of the other is sufficient to induce interactions between them to form a complex. There are ion-dipol and ion-ion interactions between PVA and PAA as well, especially in a partially neutral condition. It was also reported that PVP can be stabilized through heat treatment.[27, 28] However, whether PVP and PVP/PAA blend can form insoluble hydrogel nanofibers through a heat treatment has not been proved in the research literature yet.

Herein, we report on the preparation of PVP and PVP/PAA blend hydrogel nanofibers simply by heat treatment of the electrospun nanofibers. Without using any toxic agent for crosslinking, the nanofiber membranes showed twice larger water-swelling ratio in comparison to their film counterparts. The effects of heat-treatment temperature and PVP/PAA ratio on swelling behavior and water solubility were examined. This work may provide a simple method to prepare non-toxic hydrogel nanofibers from two widely available polymers, PVP and PAA. The hydrogel nanofibers developed are expected

find applications in the areas where bio-safety has high priority, such as biomedical, cosmetic and food industry.

Experimental

Materials

PVP (Mw ~1,300,000), PAA (Mw ~2,000), and *N,N-d*imethylformamide (DMF) were purchased from Sigma-Aldrich and used as received. PVP and PAA solutions were prepared separately by dissolving PVP or PAA powder in DMF under magnetic stirring at room temperature. The concentration of PVP and PAA solutions is 20 wt%. PVP/PAA solutions with unit ratio 8/2, 6/4 and 4/6 were produced by mixing a PVP solution with a PAA solution at room temperature, respectively. The ratio of base unit number between PVP and PAA, i.e. (number of base units for PVP)/(number of base units for PAA), in the solution was used to express the molar ratio of the two polymers.

Preparation of nanofiber membranes and films

The polymer solution was placed to a plastic syringe and then charged with a high voltage of 20 kV (ES30P, Gamma High Voltage Research) through a metal syringe needle (21 gauges). Nanofibers were electrospun at the needle tip and collected on an aluminum foil mounted onto the rotating metal drum (100 rpm). The drum was electrically ground and placed 15 cm away from the tip of the needle. The flow rate of the polymer solution was controlled at 0.8 ml/hr by a syringe pump (KD Scientific, Holliston, MA, USA). The nanofiber membranes used for further analysis were removed from aluminum foil and were about 300 μm in thickness. Finally, the as-spun nanofiber membranes were heated at temperatures of 140, 180 and 200 °C, for 1 hour each. After heating, the samples were stored in a desiccator for further characterizations.

Polymer films were prepared by casting the solution PVP and PVP/PAA to a glass Petri dish. The samples were placed in an air circulating oven at 60 °C overnight to remove DMF solvent residue and stored in a desiccator for further experiments, their thickness was about 300 μm. The polymer films were used as a control to examine the effect of nanofibrous structure on swelling and solubility properties.

Swelling behavior of nanofiber membranes

The swelling behavior was evaluated according to Japanese Industrial Standard (K8150 method). Briefly, dry nanofiber membranes (0.05~0.1 g) were immersed in DI water (30 ml) at room temperature for 30 minutes. After swelling, nanofiber membranes were filtered with a filter (0.45 □m, QTY 90 mm). Swelling ratio (*SR*) was calculated according to Eq. (1):

$$SR(g/g) = \left(\frac{w_s - w_0}{w_o}\right) \qquad (1)$$

where w_s is the weight of the nanofiber membrane after immersing in water and w_0 is the weight of the nanofiber membrane in dry state.

Solubility behavior of nanofiber membranes

Nanofiber membranes were fully dried at 60 °C for 24 hours prior to test. The extraction with DI water was performed in glass bottles which were placed on a roller mixer at room temperature overnight. The solid residual after extraction was collected using a nylon filter (0.45 □m, QTY 90mm), which was dried to constant weight (60 °C for 24 hrs).[29, 30] The insoluble part of nanofiber membranes (gel content), *g (%)*, was calculated according to Eq. 2:

$$g(\%) = \left(\frac{w_e}{w_d}\right) \times 100 \qquad (2)$$

where w_d and w_e are the weight of the dry nanofiber membrane before and after extraction, respectively.

Other characterizations of nanofiber membranes

Surface morphology of nanofiber membranes before and after swelling was observed using a scanning electron microscope (SEM, Supra 55VP, Zeiss) at an accelerating voltage of 5 kV and distance of 10 mm. Hydrogel nanofibers were dried in a vacuum oven overnight, and they are then mounted onto an Al sample holder with a conducting tape specific for SEM use. The sample surface was then sputter-coated with a thin layer of gold. Fourier transform infrared spectroscopy (FTIR) spectra were recorded on Bruker Vertex 70 spectrophotometer in ATR mode. Each spectrum with an average of 100 scans was obtained at a resolution of 4 cm^{-1} wavenumber. All tests were carried out in a controlled environment 20 ± 2 °C and 65 ± 2% relative humidity. Differential scanning calorimetry (DSC) analysis was performed on TA instruments (Q100 DSC). All nanofiber membranes were dried in an oven at 60 °C for 12 hours before testing. The test was conducted in a temperature range of 40 ~ 150 °C (ramp 10 °C/min) under a nitrogen atmosphere (flow rate, 5 ml/min). The tensile property of nanofiber membranes was tested on an Instron tensile tester at controlled environment, 20 ± 2 °C and 65 ± 2 % relative humidity. The specimens were 30 mm in length and 10 mm in width. The membrane thickness was measured using a thicknesses tester (Digimatic Indicator, Mitutoyo).

Results and discussion

Nanofiber morphology

Fig. 1 shows the SEM images of as-electrospun nanofibers. Pure PVP nanofibers appeared to be coarser than PVP/PAA nanofibers. The PAA content in PVP/PAA mixture noticeably affected the fiber uniformity. When the PVP/PAA unit ratio in the electrospinning solution changed from 8/2 to 6/4, beaded fibers were considerably reduced. The introduction of PAA in the mixed solution increased solution viscosity because of the interaction between PVP and PAA molecules, which led to the formation of uniform nanofibers. A further increase in PAA content (PVP/PAA 4/6) declined the electrospinning ability. As a result, only dense film was collected. This result could be attributed to low molecular weight of PAA which in predominance decreased final solution viscosity.

The 2nd and the 3rd lines images of Fig. 1 show nanofibers after heat treatment at 180 and 200 °C, respectively. No

significant morphology change was observed when the heat treatment was at 180 °C. When the heat treatment was around 200 °C, interconnections formed among nanofibers because nanofibers began to melt at this temperature. PVP nanofibers have an average fiber diameter over 800 nm, while the diameter of PVP/PAA nanofibers was less than 120 nm (Fig. 1e). The heat treatment increased the PVP fiber diameter, but had a little influence on the diameter of PVP/PAA fibers.

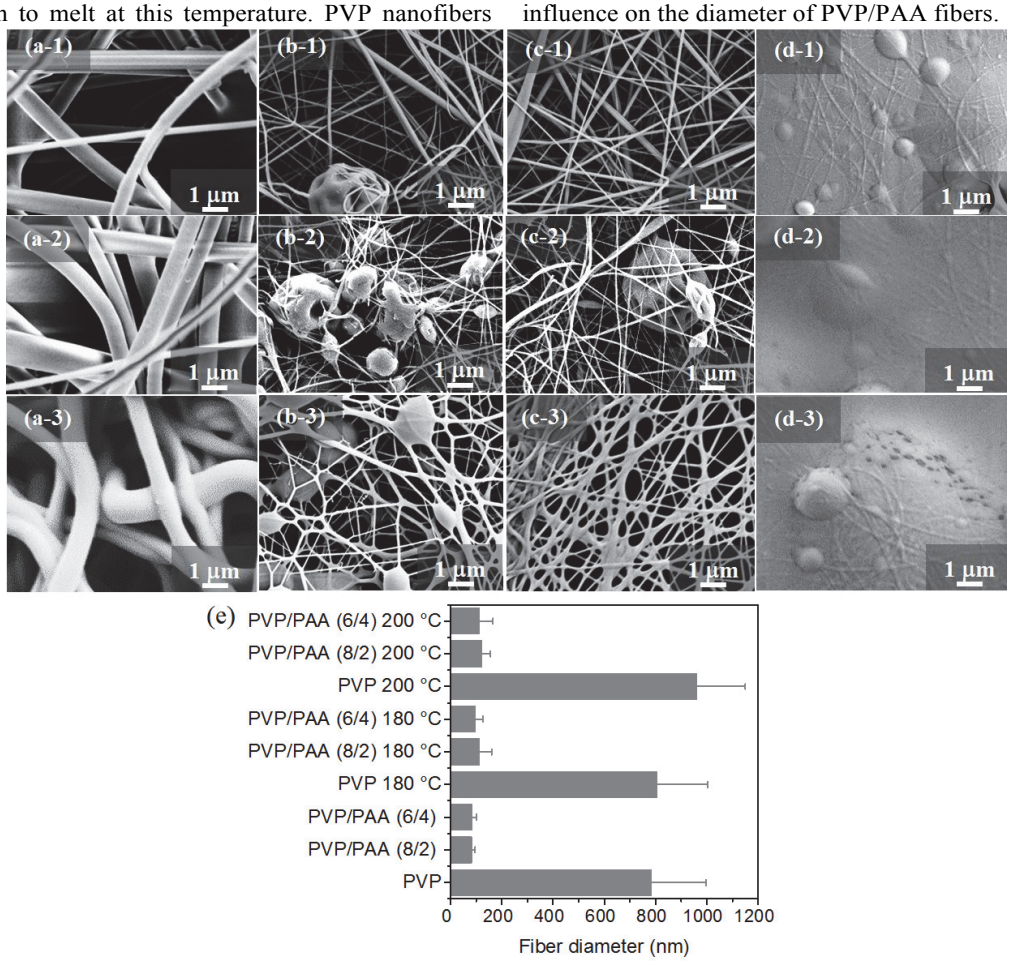

Fig. 1 SEM images of nanofibers prepared from: (a) pure PVP, (b) PVP/ PAA (unit ratio 8/2), (c) PVP/ PAA (unit ratio 6/4), (d) PVP/ PAA (unit ratio 4/6). 1st line: as-spun; 2nd line: after heating at 180 °C (1 hour); 3rd line, after heating at 200 °C (1 hour), (e) average diameter of PVP and PVP/PAA nanofibers.

FTIR spectra of nanofiber membranes

The FTIR spectra of pure PVP and PVP/PAA nanofibers are shown in Fig. 2a. The band at 1710 cm^{-1} corresponded to carbonyl stretching of carboxylic acid in PAA. The absorption band at 1660 cm^{-1} was assigned to a combined contribution from C=O and C-N stretching of PVP.[31] The peak at 1495 cm^{-1} came from the vibration of CH_2 in PVP. The spectra of the PVP/PAA fibers showed the combination of both polymers. The higher ratio of PAA led to higher intensity of carbonyl stretching band.

To better describe the composition of PVP/PAA blends, the carbonyl band in FTIR was curving fitted (Fig. 2b). The shape of the carbonyl absorption bands for PVP/PAA blends depended on the unit ratio of individual components. Little difference in the carbonyl region was observed between PVP and PVP/PAA (unit ratio 8/2). By increasing the PAA content, red shift of band at around 1640 cm^{-1} appeared which was attributed to the formation of hydrogen-bonds between the carbonyl groups in PVP and the carboxyl groups of PAA. This absorption band-shift to the lower wavenumber has been explained previously.[26, 32]

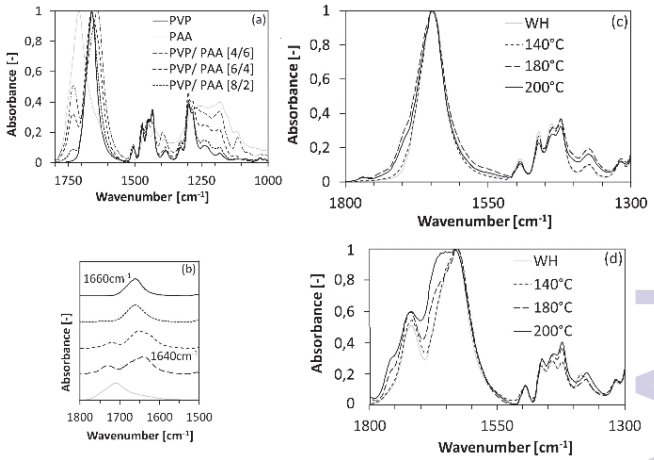

Fig. 2 FTIR spectra of (a) nanofibers with different PVP/PAA unit ratios, (b) enlarged carbonyl band of PVP, PAA and their blends, (c) pure PVP nanofibers without heat (WH) and after heat treatment, and (d) PVP/PAA (unit ratio 6/4) nanofibers WH and after heat treatment (from 140 to 200 °C).

Fig. 2c and d show the FTIR spectra of the nanofibers before and after heat treatment. In the case of PVP/PAA nanofibers (unit ratio 6/4), the small peak appeared at 1760 cm^{-1} and side peak at 1710 cm^{-1} (in Fig. 2c). This was probably due to the crosslinking of PVP, which has been reported before.[27, 28] The presence of PAA showed a little influence on the heat crosslinking reaction. (unit ratio 6/4) nanofibers, the absolute absorbance of carbonyl absorption peak at 1710 cm-1 increased with increasing the temperature.

Thermal analysis of nanofiber membranes

Fig. 3a shows DSC curves of PVP and PVP/PAA nanofibers with different unit ratios. No peaks were found to be associated with fusion or phase transition. A broad endothermic peak was observed in the temperature range between 60 °C and 100 °C, corresponding to the dehydration of PVP. In the presence of PAA, the intensity of these endothermic peaks declined. Fig. 3b shows DSC curves of PVP/PAA nanofibers (unit ratio 6/4) before and after heat treatment. Weaker endothermic peak resulted when they were treated at higher temperature. The reduced endothermic peak was attributed to the removal of certain water from the nanofiber samples after the heat treatment.

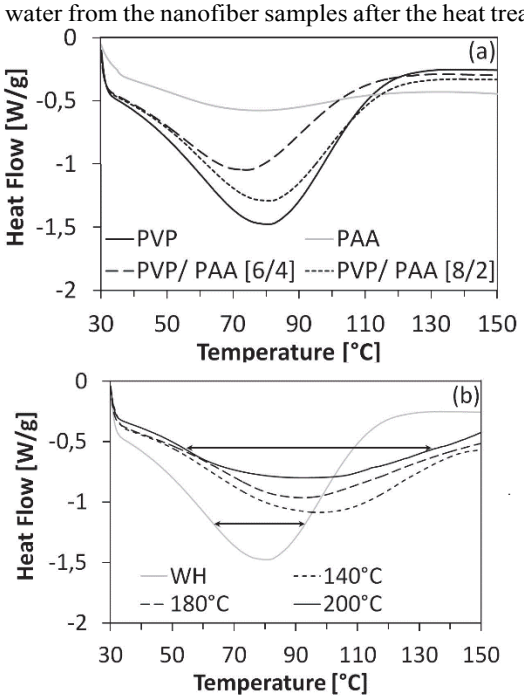

Fig. 3 DSC curves of nanofibers (a) with different PVP/PAA unit ratio, (b) PVP/PAA (unit ratio 6/4) WH and after heat treatment (from 140 to 200 °C).

Hydrogel behavior of nanofiber membranes

Before immersing in water, the heat treated PVP/PAA nanofiber membranes were white and opaque. The can be explained by the randomly orientated electrospun nanofiber structure, which forms a porous structure with strong reflection to light. In contrast, casting film looked more transparent because it has a dense structure without trapping air inside. They became transparent and swollen, after being immersed in DI water (Fig. 4). However, they remained insoluble even after immersing in water for 24 hours. Similar phenomenon was also found on PVP nanofiber membranes and films. This indicate that PVP undergoes crosslinking after heat treatment.

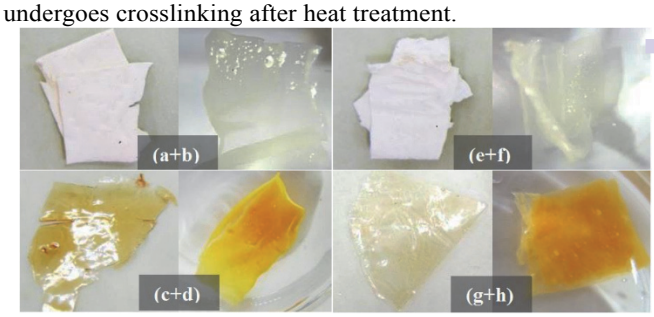

Fig. 4 Photos of PVP nanofibers (a) in dried state and (b) after swelling in water; PVP/PAA film (c) in dried state and (d) after swelling in DI water for 24 hours. Photos of PVP/PAA nanofibers (e) in dried state and f) after swelling in water; PVP film (g) in dried state and (h) after swelling in DI water for 24 hours.

Heat treatment temperature had an effect on the morphology of PVP/PAA nanofibers after immersing in water. Both PVP/PAA and PVP nanofibers after heat treatment at a temperature lower than 180 °C dissolved in water immediately due to insufficient crosslinking. For PVP/PAA nanofibers treated at 180 °C, they did not dissolve in water after 24 hours, however they failed to retain the fiber structure after immersing in water (Fig. 5, a-1~c-1). The fibers merged together to form a film. This is presumably due to insufficient crosslink. When nanofibers were treated at 200 °C, they maintained the fibrous structure after immersing in water, although they had swollen. PVP nanofibers can also retain their fiber shape after heating treatment at 200 °C (Fig. 5 a-2~c-2).

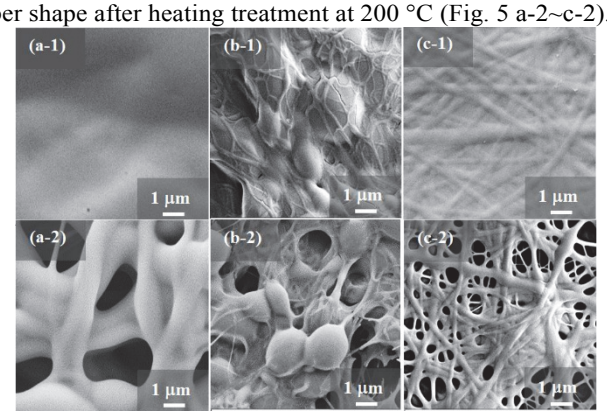

Fig. 5 SEM images of nanofibers after immersing in water. 1st line treated at 180 °C. 2nd line treated at 200 °C: (a) PVP, (b) PVP/PAA (unit ratio 8/2) and (c) PVP/PAA (unit ratio 6/4).

The unit ratio affected the morphology of PVP/PAA nanofibers after immersing in water as well. From the Fig. 5 b-2 and c-2, it is clearly seen that PVP/PAA nanofibers with unit ratio 6/4 maintained the best nanofiber structure without any beads or defects. This should come from the formation of crosslinked structure, making the PVP/PAA nanofibers retain fiber morphology (Fig. 1 c-3).

The swelling ratio is an important characteristic for hydrogel. Fig. 6 shows the swelling test results. The PVP/PAA nanofibers after heat treatment reached a swelling ratio in the range between 500% and 3700%, which was higher than that of PVP/PAA films (300% ~ 1700%). The swelling ratio did not change significantly after 10

minutes immersing in water. The swelling ratio of PVP/PAA nanofibers decreased with rising the heat temperature from 180 °C to 200 °C, because more crosslinks formed at higher temperature, which impeded the swelling of nanofibers.

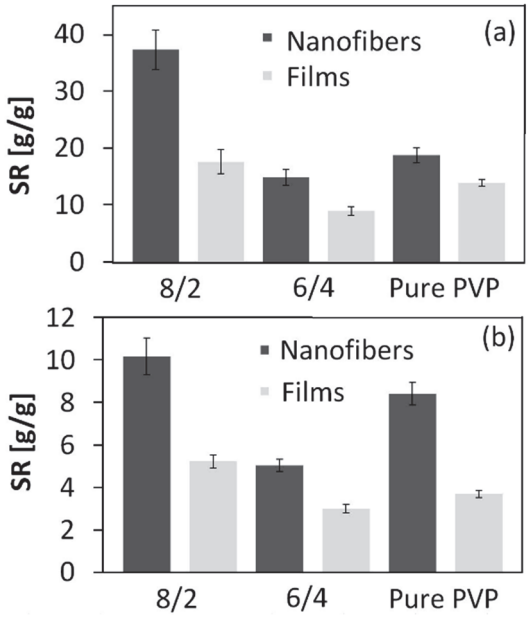

Fig. 6 Swelling ratio of PVP/PAA and PVP crosslinked nanofiber membranes and films after heat treatment for: (a) 180°C and (b) 200°C.

The unit ratio of PVP/PAA hydrogel nanofibers affected the swelling ratio. For the pure PVP nanofibers, their swelling ratio was lower than that of nanofibers with a PVP/PAA unit ratio of 8/2, but larger than those with PVP/PAA ratio of 6/4. The film PVP/PAA samples showed a similar trend. This is because of PAA in the nanofibers increases the water absorption ability. As a result, PVP absorbed less water and retained better fiber morphology. It is worth to notice that higher PAA content in nanofibers could lead to instability of the hydrogels.

The hydrogel content was estimated by immersing nanofiber membranes in DI water at room temperature for 24 hour and then measuring their dried insoluble part. When hydrogel nanofiber samples were immersed in deionized water for over 1 day, the weight of insoluble part was almost unchanged. For PVP and PVP/PAA nanofiber membranes after heat treatment at 180 °C, they exhibited considerable swelling in DI water, but remained insoluble after 24 hours. In contrast, for the un-treated nanofiber membranes and those treated at lower temperature, disintegration happened when they were placed to water. Apparently, the non-solubility resulted from heat treatment at a temperature above 180 °C. The heat treatment also made our PVP and PVP/PAA nanofibers distinct to the conventional electrospun PVP nanofibres [22~24] in water solubility and swelling feature.

Fig. 7 shows the solubility result of nanofibers and films. After immersing in DI water, the insoluble part for the heat treated PVP/PAA nanofibers reached 63% - 85% (g [%]), which increased with increasing the treatment temperature. The insoluble part decreased with increasing the PAA content in the PVP/PAA nanofibers. The insoluble part of pure PVP nanofibers reached approximately 69.5% ~ 75%, which was slightly higher than that of the PVP/PAA nanofibers with unit ratio of 6/4 but lower than PVP/PAA nanofibers with the unit ratio of 8/2. These results suggest that the heat induced crosslinking reaction mainly takes place within PVP, and the addition of a small amount of PAA to PVP improves the stability of the hydrogel nanofiber membranes in water. PVP was reported to open the pyrrolidone ring to generate amine and –COOH groups at high temperature.[32] This leads to PVP chains crosslinking with each other. When PAA is present, the reaction may be extended to the –COOH groups of PAA, allowing the PAA link up with PVP.

The insoluble part of PVP/PAA films showed a similar trend to PVP/PAA nanofibers. However, the weight ratio of insoluble part for the PVP/PAA films was lower when compared to their nanofiber counterparts at the same PVP/PAA unit ratio. This is presumably because of the highly porous feature of nanofiber membranes which facilitates water up taking.

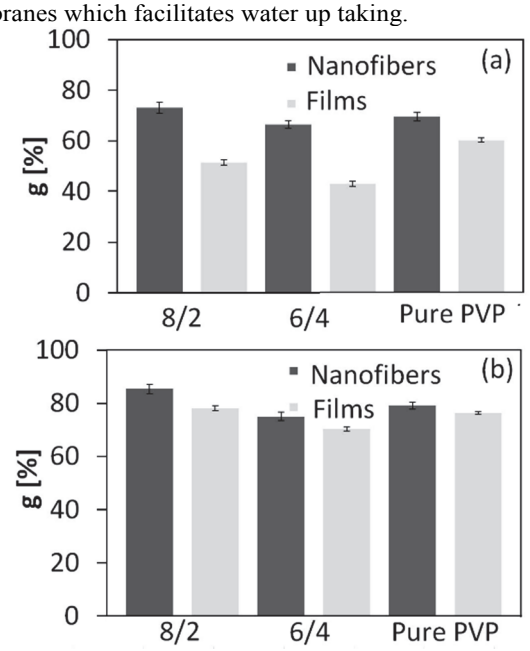

Fig. 7 The insoluble part of heat treated PVP/PAA nanofibers (g [%]) and films after immersing into water for 24 hrs. Heat treatment temperature: (a) 180 °C and (b) 200 °C.

Table 1 lists the tensile property of the nanofiber membranes. Before heat treatment, the PVP nanofiber membrane had a tensile strength of 5.5 MPa. For the PVP/PAA nanofibers, the membrane tensile strength was lower than that of the pure PVP. This could come from the low molecular weight of PAA, which weakens the PVP inter-chain interaction. The heat treatment showed an effect on the tensile strength. After heat treatment at 200 °C, these nanofibers in dry state showed improved tensile strength. The tensile strength for the PVP/PAA nanofiber membrane was 7.6 MPa and 1.1 MPa when their unit ratio was 8/2 and 6/4, respectively.

After heating treatment, the strain at break decreased for the pure PVP and the PVP/PAA (8/2) nanofiber membranes, whereas the break strain for the PVP/PAA was not changed much. This indicated that small amount of PAA in PVP increases the plasticity of the polymer blend.

Upon fully swollen with water, the heat-treated nanofiber membranes decreased the tensile strength dramatically due to the absorption of a large quantity of water. The PVP/PAA (8/2) had the

tensile strength of 0.13 MPa, while PVP/PAA (6/4) and PVP nanofiber membranes had smaller tensile strength, presumably due to the low crosslinking structure.

Table 1 Tensile property of nanofiber membranes.

Nanofiber Membranes	States	Strain at break (%)	Strength (MPa)
PVP	As-spun	15.3	5.5
	After heat[a]	18.9	8.9
	Water swollen[b]	9.6	0.005
PVP/PAA (8/2)	As-spun	16.6	2.3
	After heat[a]	29.9	7.6
	Water swollen[b]	29.1	0.13
PVP/PAA (6/4)	As-spun	10.1	1.0
	After heat[a]	10.2	1.2
	Water swollen[b]	55.1	0.089

a: Heat treatment at 200 °C; b: fully swollen in water.

The swelling repeatability of the hydrogel nanofibers was tested. As shown in Fig. 8, PVP/PAA hydrogel nanofiber membrane (e.g. unit ratio 8/2 and 6/4, treated at 200 °C) showed constant swelling ratio after 10 cycles of drying and re-swelling. For the pure PVP nanofiber membrane after heating treatment, the result of swelling repeatability cannot be obtained due to the low mechanical strength of the fiber membrane in swelling state.

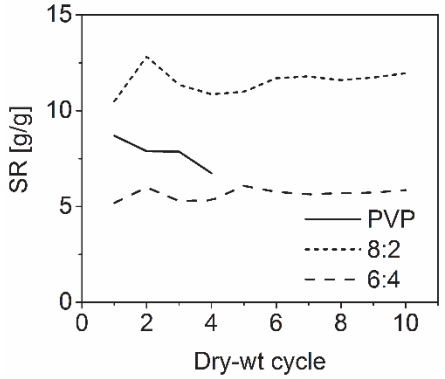

Fig. 8 Swelling ratio of PVP and PVP/PAA nanofiber membranes changing with dry-&-swelling cycles. (All nanofiber were heat treated at 200 °C)

Conclusions

PVP and PVP/PAA hydrogel nanofibers have been prepared by an electrospinning method followed by a thermal treatment. Heat treatment at a temperature above 180 °C plays a key role in forming insoluble nanofiber membranes in water. PVP/PAA unit ratio in the nanofibers affects swelling ratio and solubility. The PVP/PAA nanofibers containing a small amount of PAA show higher swelling ratio and stability in water than pure PVP nanofibers. Both pure PVP and PVP/PAA blend nanofibers have higher swelling ratio and better stability in water than their film counterparts. Since no toxic agent is used for crosslinking, PVP and PVP/PAA blend hydrogel nanofibers may find applications in the areas of cosmetic, pharmacy or wound dressings where bio-safety is pre-request to the materials.

Acknowledgements

Financial support from the Ministry of Education, Youth and Sports in the framework of National Program for Sustainability I, the OPR & DI project LO1201, Centre for Nanomaterials, Advanced Technologies and Innovation (CZ.1.05/2.1.00/01.0005), the Project Development of Research Teams of R & D Projects at the Technical University of Liberec (CZ.1.07/2.3.00/30.0024) and Deakin University for visiting scholar is acknowledged.

Notes and references

[a] *Institute for Nanomaterials, Advanced Technologies and Innovation, Technical University of Liberec, Liberec 461 17, Czech Republic;*

[b] *Institute for Frontier Materials, Deakin University, Geelong, VIC3216, Australia;*

* *Corresponding author, e-mail: tong.lin@deakin.edu.au Phone: +61 3 522 71245*

1 A. Hoffman, *Advanced Drug Delivery Reviews*, 2002, **54**, 3-12.
2 J. L. Drury and D. J. Mooney, *Biomaterials*, 2003, **24**, 4337-4351.
3 C. Liu, Z. Zhang, X. Liu, X. Ni and J. Li, *RSC Advances*, 2013, **3**, 25041-25049.
4 J. S. Boateng, K. H. Matthews, H. N. E. Stevens and G. M. Eccleston, *Journal of Pharmaceutical Sciences*, 2008, **97**, 2892-2923.
5 B. V. Slaughter, S. S. Khurshid, O. Z. Fisher, A. Khademhosseini and N. A. Peppas, *Advanced Materials*, 2009, **21**, 3307-3329.
6 M. Goldberg, R. Langer and X. Q. Jia, *Journal of Biomaterial Science-Polymer Edition*, 2007, **18**, 241-268.
7 A. Greiner and J. Wendorff, *Angewandte Chemie-International Edition*, 2007, **46**, 5670-5703.
8 D. Li and Y. Xia, *Adv. Mater.*, 2004, **16**, 1151-1170.
9 S. Ramakrishna, K. Fujihara, W. Teo, T. Yong, Z. Ma and R. Ramaseshan, *Materials Today*, 2006, **9**, 40-50.
10 D. Lubasova, A. Netravali, J. Parker and B. Ingel, *J. Nanosci. Nanotechnol.*, 2014, **14**, 4891-4898.
11 Fang Jian, Wang Xungai and L. Tong, *Nanofibers - Production, Properties and Functional Applications*, InTech, Shanghai, China, 2011.
12 L. Malinova, V. Benesova, D. Lubasova, L. Martinova, J. Roda and J. Brozek, *Functional Materials Letters*, 2011, **4**, 365-368.
13 Z. M. Huang, Y. Z. Zhang, M. Kotaki and S. Ramakrishna, *Composites Science and Technology*, 2003, **63**, 2223-2253.
14 L. Malinova, M. Stolinova, D. Lubasova, L. Martinova and J. Brozek, *European Polymer Journal*, 2013, **49**, 3135-3143.
15 J. Zhu and R. Marchant, *Expert Review of Medical Devices*, 2011, **8**, 607-626.
16 A. Cay and M. Miraftab, *J. Appl. Polym. Sci.*, 2013, **129**, 3140-3149.
17 D. Lee, J. Park, E. Lee, H. Kim and J. Lee, *Analyst*, 2013, **138**, 4786-4794.
18 K. S. Rho, L. Jeong, G. Lee, B. M. Seo, Y. J. Park, S. D. Hong, S. Roh, J. J. Cho, W. H. Park and B. M. Min, *Biomaterials*, 2006, **27**, 1452-1461.
19 J. Wang, A. Sutti, X. Wang and T. Lin, *Soft Matter*, 2011, **7**, 4364-4369.
20 P. Taepaiboon, U. Rungsardthong and P. Supaphol, *Nanotechnology*, 2006, **17**, 2317-2329.
21 L. Yang, C. F. C. Fitie, K. O. van der Werf, M. L. Bennink, P. J. Dijkstra and J. Feijen, *Biomaterials*, 2008, **29**, 955-962.
22 D. Yu, X. Shen, X. Zhang, C. Branford-White and L. Zhu, *Acta Polymerica Sinica*, 2009, 1170-1174.
23 M. Dai, A. Senecal and S. Nugen, *Nanotechnology*, 2014, **25**.
24 X. Q. Li, L. Lin, Y. N. Zhu, W. W. Liu, T. S. Yu and M. Q. G. *Polymer Composites*, 2013, **34**, 282-287.
25 R. Fogaca and L. Catalani, *Soft Materials*, 2013, **11**, 61-68.
26 H. Kaczmarek, A. Szalla and A. Kaminska, *Polymer*, 2001, **42**, 6057-6069.

27 H. T. Niu, J. Zhang, Z. L. Xie, X. G. Wang and T. Lin, *Carbon*, 2011, **49**, 2380-2388.
28 P. Q. Wang, D. Zhang, F. Y. Ma, Y. Ou, Q. N. Chen, S. H. Xie and J. Y. Li, *Nanoscale*, 2012, **4**, 7199-7204.
29 N. Peppas, Y. Huang, M. Torres-Lugo, J. Ward and J. Zhang, *Annual Review of Biomedical Engineering*, 2000, **2**, 9-29.
30 R. K. Gangwar, V. A. Dhumale, D. Kumari, U. T. Nakate, S. W. Gosavi, R. B. Sharma, S. N. Kale and S. Datar, *Materials Science and Engineering: C*, 2012, **32**, 2659-2663.
31 Y. Tan, K. Peh and O. Al-Hanbali, *Journal of Pharmacy and Pharmaceutical Sciences*, 2001, **4**, 7-14.
32 M. Yin, Y. Ye, M. Sun, N. Kang and W. Yang, *Macromol. Rapid Commun.*, 2013, **34**, 616-620.